The Astronomical Journal, 133:2209–2215, 2007 May

THE REST-FRAME *K*-BAND LUMINOSITY FUNCTION OF GALAXIES IN CLUSTERS TO $z = 1.3$

Roberto De Propris,[1,2] S. A. Stanford,[3,4] Peter R. Eisenhardt,[5,6] Brad P. Holden,[7] and Piero Rosati[8]
Received 2006 October 25; accepted 2007 January 31

ABSTRACT

We derive the rest-frame *K*-band luminosity function for galaxies in 32 clusters at $0.6 < z < 1.3$ using deep 3.6 and 4.5 μm imaging from the *Spitzer Space Telescope* Infrared Array Camera. The luminosity functions approximate the stellar mass function of the cluster galaxies. Their dependence on redshift indicates that massive cluster galaxies (to the characteristic luminosity M_K^*) are fully assembled at least at $z \sim 1.3$ and that little significant accretion takes place at later times. The existence of massive, highly evolved galaxies at these epochs is likely to represent a significant challenge to theories of hierarchical structure formation where such objects are formed by the late accretion of spheroidal systems at $z < 1$.

Key words: galaxies: evolution — galaxies: formation — galaxies: luminosity function, mass function

Online material: machine-readable table

1. INTRODUCTION

Clusters of galaxies are important for studies of galaxy formation and evolution, because they contain a *volume-limited* population of galaxies observed *at the same cosmic epoch*. They therefore provide a well-defined sample of objects to cosmologically significant look-back times whose member galaxies can be identified by simple counting statistics, without the need for extensive spectroscopic surveys or multicolor data.

One important characteristic of early-type galaxies in clusters is that they are known to follow tight color-magnitude relations, which appear to be universal and to have very small intrinsic scatter to the highest redshifts yet observed (Visvanathan & Sandage 1977; Bower et al. 1992; Stanford et al. 1995, 1998; Blakeslee et al. 2003; Lopez-Cruz et al. 2004; Holden et al. 2004; Mei et al. 2006a, 2006b). Together with the conventional interpretation of the color-magnitude relation as a mass-metallicity correlation (e.g., Trager et al. 2000), this implies that the majority of the stellar populations in early-type cluster galaxies were formed via rapid dissipative starbursts at $z > 2$. Fundamental plane studies of high-redshift cluster galaxies also support this conclusion, at least for the more massive objects (van Dokkum & Stanford 2003; Wuyts et al. 2004; Holden et al. 2005), although the low-mass galaxies seem to have undergone more extended star formation histories (Poggianti et al. 2001; Nelan et al. 2005; Jørgensen et al. 2005).

Theoretically, the existence of such massive and old galaxies at high redshift should represent a severe challenge to models where galaxies are assembled hierarchically, from a sequence of major mergers at progressively lower redshifts (see, e.g., Coles 2005, Springel et al. 2005, and Baugh 2006 for recent reviews). It is not possible, however, to exclude by spectrophotometry alone that these galaxies are assembled from subunits whose star formation has already ceased, but which are not accreted until later times (similar to the so-called dry mergers; van Dokkum et al. 1999; Tran et al. 2005). This is assumed to be the main channel by which spheroids grow at $z < 1$ in the hierarchical scenario.

On the other hand, if galaxies are formed via mergers, we should observe a steady decrease of the mean stellar mass in galaxies as we go to higher look-back times and the most massive members of the merger tree branch turn into ever smaller twigs (De Lucia et al. 2006; Maulbetsch et al. 2007). While it is generally difficult to measure galaxy masses, the *K*-band luminosity function is believed to provide an adequate surrogate (Kauffmann & Charlot 1998), as the rest-frame *H* or *K* luminosity of galaxies is seen to correlate well with stellar and even dynamical mass for local samples (Gavazzi et al. 1996; Bell & de Jong 2001) and even for high-redshift galaxies (Drory et al. 2004; Papovich et al. 2005; Caputi et al. 2006).

In our previous work (De Propris et al. 1999) we showed that the observed (ground-based) *K*-band luminosity of galaxies in clusters was consistent with pure passive evolution of objects formed at high redshift and argued that this implied that the majority of the stellar mass was completely assembled by at least $z = 0.9$. More recent luminosity function studies have essentially confirmed and extended this picture of early galaxy assembly in clusters (Kajisawa et al. 2000; Nakata et al. 2001; Massarotti et al. 2003; Kodama & Bower 2003; Toft et al. 2003, 2004; Ellis & Jones 2004; Bremer et al. 2006; Lin et al. 2006; Strazzullo et al. 2006). Andreon (2006) recently derived a composite 3.6 μm luminosity function for galaxies in clusters in the *XMM*-LSS survey (at a mean redshift of 0.5), finding that the results are consistent with the previous ground-based results.

Ideally, we would wish to carry out this experiment in the *rest-frame K* band, as even the ground-based *K* band starts to sample the rest-frame optical at $z > 1$. The *Spitzer Space Telescope* (Werner et al. 2004) Infrared Array Camera (IRAC; Fazio et al. 2004a) is now capable of obtaining panoramic ($\sim 5' \times 5'$) images at $\lambda > 3$ μm with μJy sensitivity and allows us to study the rest-frame *K*-band luminosity function of cluster galaxies at high redshift.

Here we present a study of 32 clusters up to $z = 1.3$ in both the 3.6 and 4.5 μm bands and derive the evolution of the rest-frame *K*-band galaxy luminosity function, which is a close proxy for

[1] Cerro Tololo Inter-American Observatory, La Serena, Chile.
[2] Department of Physics, University of Bristol, Bristol BS8 1TL, UK.
[3] Department of Physics, University of California, Davis, CA 95616, USA.
[4] Institute of Geophysics and Planetary Physics, Lawrence Livermore National Laboratory, Livermore, CA 94550, USA.
[5] Jet Propulsion Laboratory, Pasadena, CA 91109, USA.
[6] California Institute of Technology, Pasadena, CA 91125, USA.
[7] Lick Observatory, University of California, Santa Cruz, CA 95604, USA.
[8] European Southern Observatory, 85748 Garching, Germany.

TABLE 1
OBSERVED CLUSTERS

Cluster	R.A. (J2000.0)	Decl. (J2000.0)	Redshift	Reference
RJ 1120+43	11 20 07.5	+43 18 05.0	0.60	Romer et al. (2000)
RDCS 1634.5+5724	16 34 27.6	+57 22 51.8	0.61	Rosati et al. (1998)
RDCS 0046.3+8531	00 46 19.7	+85 31 01.3	0.62	Rosati et al. (1998)
RDCS 0440.5−1630	04 40 28.4	−16 30 08.0	0.62	Rosati et al. (1998)
RDCS 0542.8−4100	05 42 50.2	−41 00 07.0	0.64	Rosati et al. (1998)
MS 1610+66	16 10 47.8	+66 08 41.0	0.65	Gioia et al. (1990)
RDCS 1936.0−4640	19 36 06.6	−46 40 03.6	0.65	Rosati et al. (1998)
RDCS 0047.3+8506	00 47 14.8	+85 06 02.0	0.66	Rosati et al. (1998)
RDCS 2313.6+1415	23 13 34.5	+14 15 15.5	0.67	Rosati et al. (1998)
RDCS 2038.5−0125	20 38 29.1	−01 25 11.7	0.68	Rosati et al. (1998)
RDCS 2236.7−2609	22 36 42.7	−26 09 30.0	0.70	Rosati et al. (1998)
RDCS 2303.7+0846	23 02 47.5	+08 44 07.4	0.73	Rosati et al. (1998)
GHO 1322+30	13 24 48.2	+30 11 14.0	0.75	Gunn et al. (1986)
RDCS 1517.9+3127	15 17 56.3	+31 27 27.0	0.75	Rosati et al. (1998)
MS 1137+66	11 40 22.3	+66 08 15.0	0.78	Gioia et al. (1990)
RDCS 1350.8+6007	13 50 46.1	+60 07 09.5	0.80	Rosati et al. (1998)
RDCS 0035.9+8513	00 35 55.2	+85 13 20.0	0.81	Rosati et al. (1998)
RDCS 1317.4+2911	13 17 21.4	+29 11 25.0	0.81	Rosati et al. (1998)
RJ 1716+67	17 16 49.6	+67 08 30.0	0.81	Henry et al. (1997)
RDCS 0152.7−1357	01 52 43.7	−13 57 21.0	0.83	Rosati et al. (1998)
RDCS 0337.4−3457	03 37 24.7	−34 57 29.0	0.84	Rosati et al. (1998)
RJ 1226+33	12 26 54.0	+33 32 00.0	0.89	Ebeling et al. (2001)
GHO 1604+4304	16 04 23.2	+43 04 44.0	0.90	Gunn et al. (1986)
3C 184	07 39 24.5	+70 23 11.0	1.00	Deltorn et al. (1997)
MG 2019.3+1127	20 19 18.0	+11 27 10.0	1.00	Hattori et al. (1997)
RDCS 0910.7+5422	09 10 45.0	+54 22 02.0	1.11	Rosati et al. (1998)
3C 210	08 58 09.9	+27 50 52.0	1.16	J.-M. Deltorn (1996, private communication)
3C 324	15 49 48.9	+21 25 38.0	1.21	Dickinson (1995)
RDCS 1252.9−2927	12 52 54.2	−29 27 07.0	1.24	Rosati et al. (1998)
RDCS 0848.9+4452	08 48 56.2	+44 52 00.0	1.26	Rosati et al. (1998)
RDCS 0848.6+4453	08 48 34.2	+44 53 35.0	1.27	Rosati et al. (1998)
QSO 1215−00	12 15 49.8	−00 34 34.0	1.31	Liu et al. (2000)

NOTE.—Units of right ascension are hours, minutes, and seconds, and units of declination are degrees, arcminutes, and arcseconds.

the stellar mass function. We adopt the cosmological parameters $\Omega_M = 0.3$, $\Omega_\Lambda = 0.7$, and $H_0 = 70$ km s^{-1} Mpc^{-1}.

2. DATA REDUCTION AND PHOTOMETRY

The sample consists of 32 clusters at $0.6 < z < 1.3$. Data were obtained with IRAC in all four filters, using five dithered frames of 200 s each. Here we discuss observations in the 3.6 and 4.5 μm filters, which map more closely to the rest-frame K band at the redshifts of our clusters.

Table 1 shows a list of clusters and some relevant properties. Most of the sample comes from the *ROSAT* Deep Cluster Survey (RDCS; Rosati et al. 1998), while a few others derive from other X-ray or optical surveys (see the table for details), but the target selection is somewhat heterogeneous, especially for the higher redshift objects. On the other hand, De Propris et al. (2003) and Popesso et al. (2005) have shown that the B-band galaxy luminosity function does not depend on cluster properties such as the velocity dispersion, Bautz-Morgan type, or richness, and De Propris et al. (1999) found no difference in the ground-based K-band luminosity function of clusters selected by density and X-ray luminosity.

The IRAC data were reduced following standard procedures. The raw (basic calibrated) data were first corrected for known IRAC artifacts associated with bright stars (muxbleed and column pulldown). Then the *Spitzer* Science Centre MOPEX software was used to mosaic the individual frames into a registered mosaic, with cosmic rays removed. This mosaicked image for each cluster and for each band has a pixel scale which is 1.414 times smaller than the original 1.2″ IRAC pixel scale, and the orientation is rotated by ∼45°.

Photometry was carried out using the Source Extractor software (SExtractor; Bertin & Arnouts 1996). We experimented with various values for the background level and the deblending threshold, because *Spitzer* images have relatively poor angular resolution (1.7″ FWHM for stellar sources) and our fields are moderately crowded.

In order to deal with the moderate crowding, we checked that the poorer resolution of *Spitzer* data does not significantly affect our detection and photometry. We verified the detections visually, both on the original image and on the aperture image produced by SExtractor. We also compared photometry in 2″, 3″, and Kron apertures, extrapolated to total magnitudes, to check that objects were properly deblended. These tests provide confidence that our photometry is not significantly affected by the crowding, although to fully address this issue will require higher resolution imaging.

3. NUMBER COUNTS FOR CLUSTER GALAXIES

We chose to measure magnitudes in fixed 3″ (radius) apertures, which were calibrated onto the Vega system and extrapolated to infinity following Fazio et al. (2004b) to produce total magnitudes. This is done for consistency with the apertures used by Fazio et al. (2004b) to derive galaxy number counts in IRAC bands, which we use for background subtraction. We then counted

TABLE 2

NUMBER COUNTS IN CLUSTERS

Cluster	$M_{\rm lim}$ 3.6 μm	$N_{\rm total}$ 3.6 μm	$N_{\rm background}$ 3.6 μm	$N_{\rm stars}$ 3.6 μm	$N_{\rm cluster}$ 3.6 μm	$M_{\rm lim}$ 4.5 μm	$N_{\rm total}$ 4.5 μm	$N_{\rm background}$ 4.5 μm	$N_{\rm stars}$ 4.5 μm	$N_{\rm cluster}$ 4.5 μm
RJ 1120+43	17.34	120	34.6	6.4	80.0	17.32	168	71.4	6.4	90.2
CL 1634+57[a]	17.36	75	48.0	14.4	12.6	17.37	112	74.8	22.5	14.7
CL 0046+85[a]	17.37	131	52.4	35.5	43.1	17.40	177	94.6	39.0	43.4
CL 0440−16	17.23	115	47.8	15.9	51.3	17.40	138	72.0	16.5	49.5
CL 0542−41	17.40	161	47.3	26.5	87.2	17.43	189	74.7	22.3	92.0
MS 1610+66	17.45	121	49.1	12.3	59.6	17.44	170	73.2	14.2	82.6
CL 1936−46[a]	17.45	134	53.0	89.3	−8.3	17.44	164	75.1	89.2	−0.3
CL 0047+85[a]	17.49	133	53.0	38.2	44.2	17.53	147	75.1	29.3	42.6
CL 2313+14	17.53	123	58.5	14.6	49.9	17.54	148	84.8	16.5	46.8
CL 2038−01	17.57	183	58.9	14.7	109.4	17.58	191	87.4	16.6	87.0
CL 2236−26	17.64	121	58.7	10.4	51.9	17.62	150	88.4	16.4	50.0
CL 2303+08[a]	17.27	73	24.0	12.8	36.2	17.69	126	88.0	20.7	25.3
CL 1322+30	17.83	134	74.0	5.2	54.7	17.71	157	92.2	2.2	62.6
CL 1517+31[a]	17.67	105	59.0	9.7	36.3	17.71	117	69.4	9.9	37.7
MS 1137+66	17.74	126	63.7	7.1	55.2	17.77	167	94.0	7.9	65.1
CL 1350+60	17.78	139	63.7	6.3	69.0	17.79	181	95.3	7.0	78.7
CL 0035+85	17.81	154	64.4	28.2	61.4	17.82	177	96.3	30.9	49.8
CL 1317+29	17.81	114	64.7	5.3	44.0	17.82	139	95.9	5.2	37.9
RJ 1716+67	17.81	167	64.4	19.8	82.8	17.82	184	97.3	22.2	64.5
CL 0152−13	17.85	161	67.1	6.0	87.9	17.82	189	97.5	6.8	84.7
CL 0337−34[a]	17.88	106	67.7	12.8	25.5	17.84	144	97.0	14.6	32.4
RJ 1226+33	17.97	129	70.5	4.7	53.8	17.85	143	93.5	5.2	44.3
GHO 1604+4304[a]	17.97	112	69.9	11.6	30.5	17.91	132	96.2	11.8	24.0
3C 184[a]	17.16	72	57.7	11.2	3.1	17.02	51	34.6	11.3	5.1
AX J2019.3+1127[a]	17.16	146	69.8	75.6	0.6	17.02	134	35.0	98.0	1.0
CL 0910+54	17.37	59	33.7	5.8	19.5	17.12	72	38.7	5.1	28.2
3C 210	17.32	62	29.1	20.7	12.2	17.18	74	40.7	6.1	27.2
3C 324	17.43	71	35.1	8.5	27.4	17.24	73	41.6	8.7	22.7
CL 1252−29	17.41	102	35.1	15.8	39.0	17.27	93	45.9	16.0	37.1
CL 0848.9+4452[b]	17.54	39	8.6	1.7	34.7	17.30	21	11.1	1.7	9.3
CL 0848.6+4453	17.54	69	34.4	6.5	28.1	17.30	79	46.3	6.7	26
QSO 1215−00[a]	17.75	55	46.2	4.8	4.0	17.36	48	45.4	4.4	−1.8

[a] Low number counts.

[b] Only the 0.5 Mpc field cluster is off center.

objects (stars and galaxies) in 0.5 mag wide bins within a circular aperture of radius 1 Mpc, centered on the brightest cluster galaxy (where the cluster density is higher with respect to background). These systems tend to lie at or near the peak in galaxy density and the center of the X-ray isophotes. Ideally, we would wish to choose an aperture based on the cluster structural parameters (e.g., r_{200}), but the IRAC field size is not sufficiently large to derive a reliable profile for the cluster galaxy distribution. Since it is unlikely that the few bright galaxies at large clustercentric radii may affect the luminosity function parameters significantly, and since there is little evidence that the luminosity function varies with distance from the cluster center, at least for bright galaxies (De Propris et al. 2003; Lin et al. 2004; Popesso et al. 2005), our choice of a 1 Mpc aperture should not affect our conclusions.

We estimated the contribution of background galaxies to the observed counts by using the 3.6 and 4.5 μm counts of Fazio et al. (2004b). We fitted a low-order polynomial to the literature counts to smooth the effects of large-scale structure along the lines of sight of the background fields. Errors were assumed to be Poissonian, while the clustering contribution was calculated following Huang et al. (1997) and Driver et al. (2003). The Poisson errors for the cluster counts and the background contribution and the clustering errors for the field contribution were then added in quadrature as appropriate.

Because of the low resolution of the *Spitzer* data, we are not able to discriminate easily between stars and galaxies. There are no published star count models for *Spitzer* passbands. We estimated the stellar contribution using the predicted *L*-band counts from the Besançon model of the Galaxy (Robin et al. 2003). These give a good fit to the star counts reported by Fazio et al. (2004b) in the extended Groth strip and QSO 1700 fields.

Table 2 shows the raw number counts, estimated background contribution, stellar contamination, and corrected number of (statistical) cluster members to the limiting apparent magnitude we use for both IRAC bands. The limiting magnitude is designed to reach the same absolute magnitude in all clusters (in two broad redshift ranges; see discussion below), such that the cluster counts in the faintest bin are still significantly above the predicted contamination. At the same time, the brighter magnitude limit (typically around 18 mag) reduces the effect of crowding, which is most significant for the fainter galaxies. This limit is found to lie below the knee of the luminosity function and in the regime where the counts are fitted by a power law.

There are some objects for which the level of contamination from foreground stars is high or that have low number counts. These objects are identified in Table 2 and not used in our analysis. In practice, we choose objects in which the residual cluster counts (after removal of background galaxies and stars) are higher than 50 in the 3.6 μm band for the $z < 0.9$ sample (where this band is closer to the rest-frame K) and higher than 25 for the $z > 1.1$ sample in the 4.5 μm band (i.e., where this passband better probes the rest-frame K); CL 0848.9+4452 is an exception to this, as we have only one-fourth of the field of other clusters. We remark that there is no evidence for the actual existence of our highest redshift target (QSO 1215−00), suggesting that the structure identified by Liu et al. (2000) consists of a small group or filament.

The actual counts for each cluster suffer from small number statistics. Rather than recovering the luminosity function from Bayesian methods (e.g., Andreon et al. 2005) we use composite luminosity functions, in order to average errors out (cf. Andreon 2006). We create composite luminosity functions for clusters in two redshift bins, at $0.6 < z < 0.9$ and $1.1 < z < 1.3$, in both bands, following the procedure described by Colless (1989). We bin galaxies in 0.5 mag wide absolute magnitude bins in rest-frame K, adopting the cosmology specified above and a k-correction derived using the models of Bruzual & Charlot (2003) to transform from the observed IRAC bands to rest-frame K. We choose to sample these two redshift bins for the following reasons: Most previous studies, starting from De Propris et al. (1999), have studied clusters at $z < 1$; only recently have adequate cluster samples at $z > 1$ become available (e.g., Toft et al. 2003, 2004; Strazzullo et al. 2006). The two redshift bins we study sample the rest-frame K-band luminosity function of galaxies in these two regimes, i.e., both the reasonably well-studied $z < 1$ sample and the more recent clusters at higher redshift. Furthermore, the 3.6 μm band maps closely to rest-frame K for the $0.6 < z < 0.9$ interval, while the 4.5 μm band does the same for the $1.1 < z < 1.3$ regime.

TABLE 3

The k-Corrections

Redshift	$k_{3.6}$	$k_{4.5}$
0.01	−0.216	−0.216
0.025	−0.249	−0.268
0.05	−0.3	−0.352
0.075	−0.347	−0.433
0.1	−0.391	−0.512
0.125	−0.434	−0.588
0.15	−0.475	−0.66
0.175	−0.516	−0.724
0.2	−0.555	−0.779
0.225	−0.594	−0.833

Note.—Table 3 is published in its entirety in the electronic edition of the *Astronomical Journal*. A portion is shown here for guidance regarding its form and content.

The k-correction used above assumes a solar-metallicity single stellar population formed at $z = 3$ and with star formation declining exponentially with an e-folding time (τ) of 0.1 Gyr, and it is computed independently for each *Spitzer* band, which is thus transformed to rest-frame K. This is done (rather than more complex approaches using both IRAC bands to derive the rest-frame K luminosity) to present the data more directly and with a minimum of model dependencies. The k-corrections used are presented in Table 3. We experimented with several "reasonable" values of τ from instantaneous star formation to 1 Gyr e-folding time bursts and found that this makes little difference to the actual value of the k-correction.

The resulting composite luminosity functions are fitted with a Schechter function, using a downhill simplex algorithm. Figure 1 shows the data in each bin and the best-fitting luminosity functions. Table 4 shows the derived M_K^* values for the luminosity function in both bands. The errors in M^* are marginal 1 σ errors derived by fixing the values of all other parameters at their "best" value. The derived α is also shown in Table 4, but we caution that the fit to the faint-end slope is very uncertain.

4. DISCUSSION

Figure 2 shows the rest-frame K-band M^* for our composite clusters, together with previous ground-based K-band data, corrected to rest-frame K following the same procedure as above, and a Bruzual & Charlot (2003) model, with solar metallicity (Salpeter initial mass function and Padova 1994 isochrones, as recommended by Bruzual & Charlot 2003) and variable formation epoch, with $\tau = 0.1$ Gyr. The actual choice of τ makes a difference only to the level of a few hundreds of magnitudes. Note that we are not attempting to actually fit models to the data

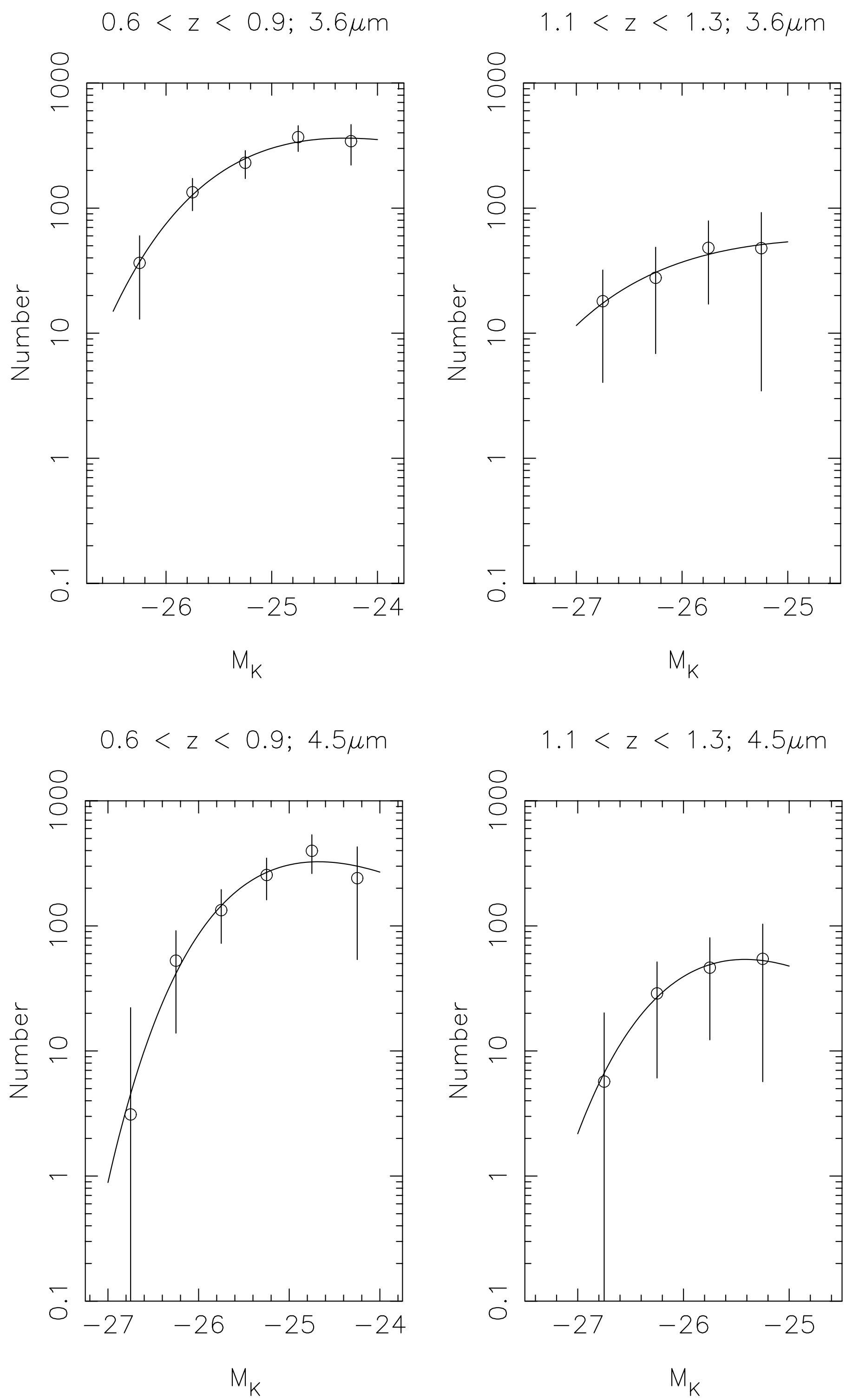

FIG. 1.—Composite galaxy luminosity functions for cluster galaxies at $0.6 < z < 0.9$ and $1.1 < z < 1.3$ in *Spitzer* 3.6 and 4.5 μm bands and best fits to a Schechter function.

shown in Figure 2, but we are showing models with representative star formation histories to obtain upper limits to the epoch of mass assembly for these cluster galaxies.

The results shown in Figure 2 imply that the majority of the stellar mass in elliptical galaxies is already assembled at least at $z = 1.3$; this is a strong upper limit to the epoch of galaxy formation in that the majority of the merger episodes (if any) must have taken place prior to this epoch. Taken at face value, these *Spitzer* data may indicate that the epoch of star formation in these objects is somewhat more recent ($1.5 < z < 2$) than indicated by some previous studies of the color-magnitude relation (Stanford et al. 1995, 1998; Blakeslee et al. 2003; Holden et al. 2004, 2006; Mei et al. 2006a, 2006b) and the fundamental plane (Wuyts et al. 2004, but see Jørgensen et al. 2005). This may be due to the fact that, at $\sim M^*$, the population includes a fraction of lenticular galaxies, whose star formation histories are more extended than the brighter elliptical galaxies. Otherwise, our results are consistent with recent work (e.g., Holden et al. 2006) showing that massive ellipticals are in place at $z \sim 1$ but are more general, as we make no morphological selection.

TABLE 4
Luminosity Function Parameters

Redshift	M^* (3.6 μm)	α	M^* (4.5 μm)	α
0.75	-24.63 ± 0.22	-0.25	-24.48 ± 0.31	0.21
1.15	-26.18 ± 1.20	-0.82	-24.83 ± 0.83	0.81

The latest hierarchical models (e.g., De Lucia et al. 2006), including AGN feedback, succeed in pushing back the epoch of major star formation to $z > 2$ for the most massive objects, but they still require most of the actual mass assembly to take place through dry mergers at later epochs; 50% of the mass in more massive galaxies ($M > 10^{11}\ M_\odot$) is assembled at $z < 0.8$, while the lower mass objects ($M > 4 \times 10^9\ M_\odot$) may be formed at higher redshifts. This is not what we observe here, where the vast majority of the stellar mass in massive (approximately L^* or greater, equivalent to a mass of $\sim 10^{11.8}\ M_\odot$, using the calibration shown in Gavazzi et al. [1996], which corresponds more closely to the virial mass; using stellar masses, this is approximately $10^{11.3}\ M_\odot$) galaxies appears to be in place at $z = 1.3$.

One possible caveat is that the theoretical models refer to the average "field" environment, while we are observing massive clusters where the main process of hierarchical merging and collapse may have taken place at earlier epochs, as they lie in overdense regions. However, Maulbetsch et al. (2007) use a high-resolution *N*-body simulation to simulate how the mass assembly histories of galaxy-size halos depend on environment and show that at $z = 1$ the mass aggregation rate is 4 times higher than at present and independent of environment, while galaxies in the densest (cluster-like) environments at $z > 1$ undergo more rapid mass accretion. This suggests that we should be witnessing a much stronger evolution of the mean galaxy mass than observed here, even for cluster environments.

Our results are therefore largely inconsistent with the hierarchical picture. Not only are the stellar populations of these galaxies formed at high redshift (see § 1), but they are also assembled into galaxies at comparatively high look-back times, arguing that star formation takes place in situ, in a manner reminiscent of the earlier monolithic collapse picture. Recently, it has been shown that this behavior largely holds for field ellipticals as well, at least to $z \sim 0.65$ (Roseboom et al. 2006; Wake et al. 2006). Similarly, *K*-selected studies in the field have also found a similar antihierarchical behavior (e.g., Cimatti et al. [2004] from the K20 survey; see also the review by Renzini [2006] for the observed "top-down" buildup of massive ellipticals, as opposed to the theoretically favored "bottom-up" scenario).

Because the power spectrum of density fluctuations in the universe at the time of recombination is tilted to low masses in the ΛCDM scenario, hierarchical accretion is a necessary consequence of the hypothesis that galaxies are formed within cold dark matter halos. The evidence presented here poses a severe challenge to the hierarchical formation scenario in that the observations show behavior *opposite* of that of the theoretical predictions, with the more massive galaxies being already present at a look-back time of 65% of the Hubble time.

We would like to acknowledge the anonymous referee for an informative report that helped make the paper clearer. We also thank Steve Willner for some comments on this paper. This work is based on observations made with the *Spitzer Space Telescope*, which is operated by the Jet Propulsion Laboratory, California Institute of Technology, under a contract with NASA. R. D. P. acknowledges support from a PPARC grant while at the University of Bristol. S. A. S.'s work was performed under the auspices of the US Department of Energy, National Nuclear Security Administration, by the University of California, Lawrence Livermore National Laboratory, under contract W-7405-Eng-48.

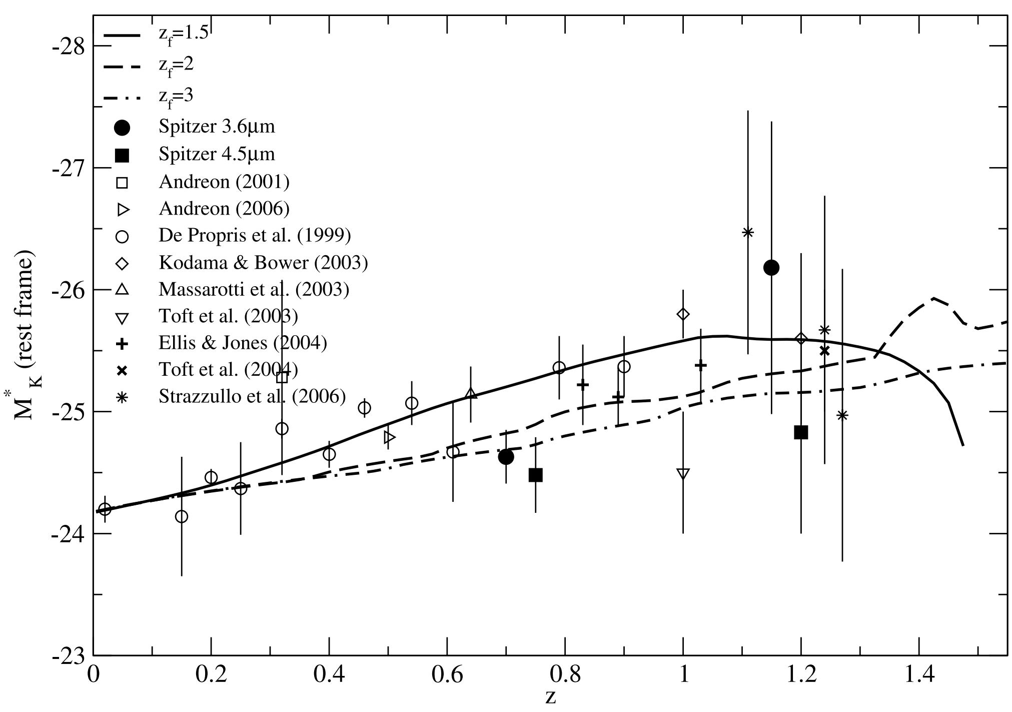

Fig. 2.—Rest-frame M_K^* from our data (*filled symbols*) in the 3.6 and 4.5 μm bands (arbitrarily shifted by 0.05 in z for clarity), together with previous *K*-band studies (as identified in the figure legend) and models from Bruzual & Charlot (2003) with z_f as indicated in the legend and $\tau = 0.1$ Gyr. The models are normalized to the value of K^* in the Coma Cluster (De Propris et al. 1998).

REFERENCES

Andreon, S. 2006, A&A, 448, 447
Andreon, S., Punzi, G., & Grado, A. 2005, MNRAS, 360, 727
Baugh, C. M. 2006, Rep. Prog. Phys., 69, 3101
Bell, E. F., & de Jong, R. S. 2001, ApJ, 550, 212
Bertin, E., & Arnouts, S. 1996, A&AS, 117, 393
Blakeslee, J. P., et al. 2003, ApJ, 596, L143
Bower, R. G., Lucey, J. R., & Ellis, R. S. 1992, MNRAS, 254, 601
Bremer, M. N., et al. 2006, MNRAS, 371, 1427
Bruzual, G., & Charlot, S. 2003, MNRAS, 344, 1000
Caputi, K. I., et al. 2006, ApJ, 637, 727
Cimatti, A., et al. 2004, Nature, 430, 184
Coles, P. 2005, Nature, 433, 248
Colless, M. M. 1989, MNRAS, 237, 799
Deltorn, J.-M., Le Fevre, O., Crampton, D., & Dickinson, M. 1997, ApJ, 483, L21
De Lucia, G., Springel, V., White, S. D. M., Croton, D., & Kauffmann, G. 2006, MNRAS, 366, 499
De Propris, R., Eisenhardt, P. R., Stanford, S. A., & Dickinson, M. 1998, ApJ, 503, L45
De Propris, R., Stanford, S. A., Eisenhardt, P. R., Dickinson, M., & Elston, R. 1999, AJ, 118, 719
De Propris, R., et al. 2003, MNRAS, 342, 725
Dickinson, M. 1995, in Galaxies in the Young Universe, ed. H. Hippelein, K. Meisenheimer, & H.-J. Röser (Berlin: Springer), 144
Driver, S. P., Odewahn, S. C., Echevarria, L., Cohen, S. H., Windhorst, R. A., Phillipps, S., & Couch, W. J. 2003, AJ, 126, 2662
Drory, N., Bender, R., Feulner, G., Hopp, U., Maraston, C., Snigula, J., & Hill, G. J. 2004, ApJ, 608, 742
Ebeling, H., Jones, L. R., Fairley, B. W., Perlman, E., Scharf, C., & Horner, D. 2001, ApJ, 548, L23
Ellis, S. C., & Jones, L. R. 2004, MNRAS, 348, 165
Fazio, G. G., et al. 2004a, ApJS, 154, 10
———. 2004b, ApJS, 154, 39
Gavazzi, G., Pierini, D., & Boselli, A. 1996, A&A, 312, 397
Gioia, I. M., Maccacaro, T., Schild, R. E., Wolter, A., Stocke, J. T., Morris, S. L., & Henry, J. P. 1990, ApJS, 72, 567
Gunn, J. E., Hoessel, J. G., & Oke, J. B. 1986, ApJ, 306, 30
Hattori, M., et al. 1997, Nature, 388, 146
Henry, J. P., et al. 1997, AJ, 114, 1293
Holden, B. P., Stanford, S. A., Eisenhardt, P. R., & Dickinson, M. 2004, AJ, 127, 2484
Holden, B. P., et al. 2005, ApJ, 620, L83
———. 2006, ApJ, 642, L123
Huang, J.-S., Cowie, L. L., Gardner, J. P., Hu, E. M., Songaila, A., & Wainscoat, R. J. 1997, ApJ, 476, 12
Jørgensen, I., Bergmann, M., Davies, R., Barr, J., Takamiya, M., & Crampton, D. 2005, AJ, 129, 1249
Kajisawa, M., et al. 2000, PASJ, 52, 61
Kauffmann, G., & Charlot, S. 1998, MNRAS, 297, L23
Kodama, T., & Bower, R. G. 2003, MNRAS, 346, 1
Lin, Y.-T., Mohr, J. J., Gonzalez, A. H., & Stanford, S. A. 2006, ApJ, 650, L99
Lin, Y.-T., Mohr, J. J., & Stanford, S. A. 2004, ApJ, 610, 745
Liu, M. C., Dey, A., Graham, J. R., Bundy, K. A., Steidel, C., Adelberger, K., & Dickinson, M. 2000, AJ, 119, 2556
Lopez-Cruz, O., Barkhouse, W., & Yee, H. K. C. 2004, ApJ, 614, 679
Massarotti, M., Busarello, G., La Barbera, F., & Merluzzi, P. 2003, A&A, 404, 75
Maulbetsch, C., Avila-Reese, V., Colín, P., Gottlöber, S., Khalatyan, A., & Steinmetz, M. 2007, ApJ, 654, 53
Mei, S., et al. 2006a, ApJ, 639, 81
———. 2006b, ApJ, 644, 759
Nakata, F., et al. 2001, PASJ, 53, 1139
Nelan, J., et al. 2005, ApJ, 632, 137
Papovich, C., et al. 2005, ApJ, 640, 92
Poggianti, B. M., et al. 2001, ApJ, 563, 118
Popesso, P., Böhringer, H., Voges, W., & Romaniello, M. 2005, A&A, 433, 415
Renzini, A. 2006, ARA&A, 44, 141
Robin, A. C., Reylé, S., Derrière, S., & Picaud, S. 2003, A&A, 409, 523
Romer, A. K., et al. 2000, ApJS, 126, 209
Rosati, P., della Ceca, R., Norman, C., & Giacconi, R. 1998, ApJ, 492, L21
Roseboom, I., et al. 2006, MNRAS, 373, 349
Springel, V., et al. 2005, Nature, 435, 629
Stanford, S. A., Eisenhardt, P. R., & Dickinson, M. 1995, ApJ, 450, 512
———. 1998, ApJ, 492, 461
Strazzullo, V., et al. 2006, A&A, 450, 909
Toft, S., Soucail, G., & Hjorth, J. 2003, MNRAS, 344, 337
Toft, S., et al. 2004, A&A, 422, 29
Trager, S., Faber, S., Worthey, G., & Gonzalez, J. 2000, AJ, 120, 165
Tran, K.-V. H., van Dokkum, P. G., Franx, M., Illingworth, G. D., Kelson, D. D., & Förster-Schreiber, N. M. 2005, ApJ, 627, L25
van Dokkum, P. G., & Stanford, S. A. 2003, ApJ, 585, 78
van Dokkum, P. G., et al. 1999, ApJ, 520, L95
Visvanathan, N., & Sandage, A. 1977, ApJ, 216, 214
Wake, D. A., et al. 2006, MNRAS, 372, 537
Werner, M. W., et al. 2004, ApJS, 154, 1
Wuyts, S., van Dokkum, P. G., Kelson, D. D., Franx, M., & Illingworth, G. D. 2004, ApJ, 605, 677